Numerical implementation of moment-kinetic electrons

M. Barnes[1], M. R. Hardman[2], S. Newton[3], J. Omotani[3] and F. I. Parra[4]

[1] Rudolf Peierls Centre for Theoretical Physics, University of Oxford, Clarendon Laboratory, Parks Road, Oxford OX1 3PU, United Kingdom
[2] Tokamak Energy Ltd, 173 Brook Drive, Milton Park, Abingdon OX14 4SD, United Kingdom
[3] Culham Centre for Fusion Energy, Culham Science Centre, Abingdon, Oxon, OX14 3DB, United Kingdom
[4] Princeton Plasma Physics Laboratory, P.O. Box 451, Princeton, New Jersey 08540, United States

E-mail: michael.barnes@physics.ox.ac.uk

1. Introduction

Calculation of the electrostatic potential is a challenge within the drift kinetic approximation. This is because, without further manipulation of the drift kinetic system of equations, there is no explicit equation to be solved for the potential: Instead, it appears as a parameter in the drift kinetic equations for both electrons and ions, which are then related to one another via quasineutrality. In report 2047357-TN-07-01 [1], we showed how the electrostatic potential could be calculated self-consistently for a 2D drift kinetic model with a helical magnetic field and with wall boundary conditions appropriate for open field lines. Considerable care had to be taken to obtain an expression for the electrostatic potential. In particular, a set of fluid equations had to be formulated for the electron dynamics, with closure via coupling to the kinetic equation for a modified electron particle distribution function. In this moment-kinetic formulation, the parallel electron momentum equation becomes the equation for the electrostatic potential, with an additional complication that the boundary value for the potential must be determined implicitly as it enters in the limits of integration for the parallel current at the plasma boundary.

Thus far we have mostly side-stepped the issue of calculating the potential in our ProxyApps by using a Boltzmann response for the electron dynamics so that no electron equations need to be solved at all. In report 2070839-TN-04, we made a start on addressing this limitation by implementing electron fluid equations for the 1+1D system described in report 2047357-TN-05-01 [2], with a Braginskii fluid closure for the electrons [3]. In this report we describe our numerical implementation of a moment-kinetic closure for the electron fluid equations.

To begin we will provide a brief overview of the physical system we aim to model, and provide the system of evolution equations for the various plasma species. At present, we are unable to obtain steady-state solutions for the electron distribution function: We provide illustrative examples of the difficulties we have encountered and discuss possible causes of and solutions to the problems observed.

2. Drift kinetic system of equations

We consider a plasma consisting of a single ion species of charge e and mass m_i, a single neutral species with mass $m_n = m_i$, and electrons with charge $-e$ and mass m_e. The plasma is immersed in a straight, homogeneous magnetic field of the form

$$\mathbf{B} = B\hat{\mathbf{z}}, \tag{1}$$

where z is the field-aligned coordinate, and $\hat{\mathbf{z}}$ is the unit vector in the direction of ∇z. We assume that the plasma is electrostatic and that the magnetic field terminates at each end on a conducting wall. The spatial domain we consider is $z \in [z_-, z_+]$, with $z_+ - z_- = L_z$. The boundaries of the domain in z are assumed to be the entrances to the magnetic pre-sheath.

We restrict our attention to parallel dynamics only and define the marginalised distribution function

$$f_s(z, v_\parallel, t) \doteq \left\langle \hat{f}_s(z, v_\parallel, v_\perp, \vartheta, t) \right\rangle \doteq 2\pi \int_0^\infty dv_\perp v_\perp \hat{f}_s, \tag{2}$$

with $\hat{f}_s$ the particle distribution function for species s, t the time, $v_\parallel$ the parallel component of the particle velocity $\mathbf{v}$, and the angle brackets denoting integration over gyro-angle ϑ and the perpendicular component of the particle velocity $v_\perp$. To facilitate this one-dimensional treatment of the velocity space, we neglect collisions between charged particles and elastic electron-neutral collisions, as the associated operators would introduce non-trivial dependence on $v_\perp$ into the electron drift kinetic equation.

As described in, e.g., Report 2047537-TN-05-1 [2], the drift kinetic equations describing the evolution of the marginalised particle distribution f_s for the ions, electrons and neutrals are

$$\frac{\partial f_i}{\partial t} + v_\parallel \frac{\partial f_i}{\partial z} - \frac{e}{m_i}\frac{\partial \phi}{\partial z}\frac{\partial f_i}{\partial v_\parallel} = -R_{\text{in}}\left(n_n f_i - n_i f_n\right) + R_{\text{ion}} n_e f_n + S_i \tag{3}$$

$$\frac{\partial f_e}{\partial t} + v_\parallel \frac{\partial f_e}{\partial z} + \frac{e}{m_e}\frac{\partial \phi}{\partial z}\frac{\partial f_e}{\partial v_\parallel} = C_{e,\text{ion}}[f_e, f_n] + S_e, \tag{4}$$

and

$$\frac{\partial f_n}{\partial t} + v_\parallel \frac{\partial f_n}{\partial z} = R_{\text{in}}\left(n_n f_i - n_i f_n\right) - R_{\text{ion}} n_e f_n + S_n, \tag{5}$$

where ϕ is the electrostatic potential, $n_s = \int dv_\parallel f_s$ is the particle density, $S_s = \left\langle \hat{S}_s \right\rangle$ is a marginalised source accounting for, e.g., heating and fueling, R_{in} and R_{ion} are constants

that determine the ion-neutral charge exchange and ionisation rates, respectively, and $C_{e,\mathrm{ion}}$ is an operator accounting for the effect on electrons of ionisation collisions. The distribution functions f_i and f_e are related to one another via quasineutrality:

$$n_i = \int_{-\infty}^{\infty} dv_\parallel f_i = \int_{-\infty}^{\infty} dv_\parallel f_e = n_e. \tag{6}$$

One of the main challenges in solving this system of equations is that there is no explicit equation for the electrostatic potential. If one were to try, e.g., to solve the ion and electron drift kinetic equations (3)-(4) using an explicit time advance algorithm with ϕ at the previous time level as an input, then in general the solutions for f_i and f_e so obtained would not satisfy Eq. (6). This procedure could be iterated, with ϕ varied until quasineutrality were satisfied, or one could develop an approach that guarantees satisfaction of quasineutrality from the outset. We have presented two such approaches in previous reports: The first assumes a Boltzmann electron response and thus avoids entirely the need to solve for the electron dynamics, while the second uses a novel moment-kinetic approach in which the electron parallel momentum equation can be used to solve for the potential explicitly while enforcing quasineutrality. In this report we describe the numerical implementation and testing of the moment-kinetic treatment for electrons.

We will assume in this report that f_i and f_n can be obtained, provided ϕ, either via direct solution of the above drift kinetic equations or via the moment-kinetic approach derived in report 2047357-TN-05-01 [2]. Our focus here will be on describing the numerical treatment of the moment-kinetic electron equations and their relationship to the calculation of the electrostatic potential.

3. Electron fluid equations

Electron fluid equations are obtained by taking the appropriate velocity moments of the electron drift kinetic equation (4) and expanding in the small parameter m_e/m_i. Details can be found in [2]. The electron continuity equation is‡

$$\frac{\partial n_e}{\partial t} + \frac{\partial n_e u_e}{\partial z} = n_e n_n R_{\mathrm{ion}} + \int_{-\infty}^{\infty} dv_\parallel S_e, \tag{7}$$

where the parallel flow of species s is given by

$$u_s \doteq \frac{1}{n_s} \int_{-\infty}^{\infty} dv_\parallel v_\parallel f_s. \tag{8}$$

The charge conservation equation, obtained by combining the electron and ion continuity equations and enforcing quasineutrality, is

$$\frac{\partial}{\partial z} \left(n_e \left(u_i - u_e \right) \right) = 0. \tag{9}$$

‡ Here we have corrected a typo in the sign of the electron ionisation particle source appearing in [2].

Note that we have assumed $\int d^3v\,(S_i - S_e)$ is small to obtain the above result. The electron parallel momentum equation is (after using $m_e/m_i \ll 1$)

$$-\frac{\partial p_{\parallel,e}}{\partial z} + en_e\frac{\partial \phi}{\partial z} = 0, \tag{10}$$

where $p_{\parallel,e}$ is the electron parallel pressure,

$$p_{\parallel,e} \doteq \int dv_\parallel\; m_e\hat{w}_\parallel^2 f_e, \tag{11}$$

and $\hat{w}_\parallel \doteq v_\parallel - u_e \approx v_\parallel$ is the parallel component of the electron peculiar velocity. The time derivative term and the term proportional to S_e have been neglected in (10) as small in m_e/m_i because we order $\partial/\partial t \sim v_{\mathrm{th,i}}/L_z$ and $S_e \sim f_e v_{\mathrm{th,i}}/L_z$, with $v_{\mathrm{th,i}} \doteq \sqrt{2T_i/m_i}$ and $T_s \doteq p_{\parallel,s}/n_s$.

Finally, the electron parallel energy equation is

$$\frac{\partial p_{\parallel,e}}{\partial t} + \frac{\partial q_{\parallel,e}}{\partial z} + u_e\frac{\partial p_{\parallel,e}}{\partial z} + 3p_{\parallel,e}\frac{\partial u_e}{\partial z} = n_n R_{\mathrm{ion}}\left(p_{\parallel,e} - n_e E_{\mathrm{ion}}\right) + \mathcal{S}_{p,e}, \tag{12}$$

where $q_{\parallel,e}$ is the electron parallel heat flux,

$$q_{\parallel,e} \doteq \int d\hat{w}_\parallel m_s\hat{w}_\parallel^3 f_e, \tag{13}$$

$\mathcal{S}_{p,e} = \int dv_\parallel m_e\hat{w}_\parallel^2 S_e$ is the electron heat source, and we have used the simple model

$$\int dv_\parallel m_e\hat{w}_\parallel^2 C_{e,\mathrm{ion}}[f_e, f_n] \doteq n_n R_{\mathrm{ion}}\left(p_{\parallel,e} - n_e E_{\mathrm{ion}}\right) \tag{14}$$

for the ionisation source, with E_{ion} the ionisation energy cost (including radiation from excited states).

The set of fluid equations (9), (10), (12) and (13) require some form of closure to calculate the parallel heat flux. We use a 1+1D version of the modified electron kinetic equation derived in [2] as our closure:

$$\dot{z}\frac{\partial g_e}{\partial z} + \dot{w}_\parallel\frac{\partial g_e}{\partial w_\parallel} = G, \tag{15}$$

where

$$w_\parallel \doteq \frac{v_\parallel - u_e}{v_{\mathrm{th,e}}} \approx \frac{v_\parallel}{v_{\mathrm{th,e}}}, \tag{16}$$

is the normalised, parallel component of the electron peculiar velocity,

$$g_e \doteq f_e\frac{v_{\mathrm{th,e}}}{n_e} \tag{17}$$

is a modified particle distribution function for the electrons,

$$\dot{z} = w_\parallel v_{\mathrm{th,e}}, \tag{18}$$

$$\dot{w}_\parallel = \frac{1}{m_e n_e v_{\mathrm{th,e}}} \frac{\partial p_{\parallel,e}}{\partial z} + \frac{w_\parallel}{2p_{\parallel,e}} \frac{\partial q_{\parallel,e}}{\partial z} - w_\parallel^2 \frac{\partial v_{\mathrm{th,e}}}{\partial z}, \tag{19}$$

and

$$G = \left(-\frac{1}{2p_{\parallel,e}} \frac{\partial q_{\parallel,e}}{\partial z} - w_\parallel v_{\mathrm{th,e}} \left(\frac{\partial \ln n_e}{\partial z} - \frac{\partial \ln v_{\mathrm{th,e}}}{\partial z} \right) \right) g_e. \tag{20}$$

With the definition (17), the modified distribution function g_e satisfies the following integral constraints:

$$\int dw_\parallel \left(1, w_\parallel, w_\parallel^2\right) g_e = \left(1, 0, \frac{1}{2}\right). \tag{21}$$

The set of equations (3), (5), (6), (9), (10), (12), and (15) constitute a closed set of equations for f_i, f_n, ϕ, n_e, u_e, $p_{\parallel,e}$, and g_e, provided an appropriate set of boundary conditions. We turn our attention to these boundary conditions next.

4. Boundary conditions

To ensure uniqueness of our solution, we must specify boundary conditions in z on the ion and neutral particle distributions, the modified electron particle distribution (17), and on the electron parallel flow and pressure. For the ions, we assume that all ions that reach the end of the domain escape to the wall, where they recombine. Thus, no ions return; i.e.,

$$f_i(z_+, v_\parallel < 0, t) = 0, \tag{22}$$

and

$$f_i(z_-, v_\parallel > 0, t) = 0. \tag{23}$$

Neutrals that leave the domain are assumed to hit the wall and thermalise at the temperature of the wall, T_w. Ions that recombine at the wall also re-enter as neutrals. The resulting boundary condition on the neutrals is

$$f_n(z_-, v_\parallel > 0, t) = \Gamma_- f_{Kw}(v_\parallel), \tag{24}$$

and

$$f_n(z_+, v_\parallel < 0, t) = \Gamma_+ f_{Kw}(v_\parallel), \tag{25}$$

where

$$f_{Kw}(v_\parallel) \doteq 3\sqrt{\pi} \left(\frac{m_i}{2T_w} \right)^{3/2} \left| v_\parallel \right| \operatorname{erfc}\left(\sqrt{\frac{m_i}{2T_w}} \left| v_\parallel \right| \right) \tag{26}$$

is the (marginalised) Knudsen cosine distribution [4], and

$$\Gamma_- \doteq \sum_{s=i,n} \int_{-\infty}^{0} dv_\parallel \left| v_\parallel \right| f_s(z_-, v_\parallel, t) \tag{27}$$

and

$$\Gamma_+ \doteq \sum_{s=i,n} \int_{0}^{\infty} dv_\parallel \left| v_\parallel \right| f_s(z_+, v_\parallel, t) \tag{28}$$

are the combined fluxes of neutrals and ions towards the walls at $z = z_-$ and $z = z_+$, respectively.

For electrons that leave the domain, their parallel energy $\mathcal{E}_\parallel = m_e v_\parallel^2/2 - e\phi$ is conserved. As a result, electrons with parallel speeds greater than $v_{c,+} \doteq \sqrt{2e(\phi(z_+,t) - \phi_w)/m_e}$ at z_+ reach the wall, with ϕ_w the potential of the wall beyond $z = z_+$; electrons with speeds less than $v_{c,+}$ are repelled back into the domain:

$$g_e(z_+, v_\parallel < 0, t) = \begin{cases} g_e(z_+, -v_\parallel, t), & |v_\parallel| < v_{c,+} \\ 0, & |v_\parallel| > v_{c,+}. \end{cases} \tag{29}$$

The boundary condition at $z = z_-$ is similar:

$$g_e(z_-, v_\parallel > 0, t) = \begin{cases} g_e(z_-, -v_\parallel, t), & |v_\parallel| < v_{c,-} \\ 0, & |v_\parallel| > v_{c,-}, \end{cases} \tag{30}$$

where $v_{c,-} \doteq \sqrt{2e\phi(z_-,t)/m_e}$, and we have chosen ϕ to be zero at the wall beyond z_-. Note that while we have formulated the boundary conditions in terms of $v_\parallel$, the fact that $u_e \sim u_i \ll v_{\mathrm{th,e}}$ implies that $v_\parallel \approx w_\parallel v_{\mathrm{th,e}}$.

Integrating the charge conservation equation (9) and using (29)-(30) gives a constraint on the parallel current at the domain boundaries:

$$\begin{aligned} 0 = J_\parallel(z_+,t) - J_\parallel(z_-,t) = &\int_0^\infty dv_\parallel v_\parallel f_i(z_+, v_\parallel, t) - \int_{v_{c,+}}^\infty dv_\parallel v_\parallel f_e(z_+, v_\parallel, t) \\ &- \int_{-\infty}^0 dv_\parallel v_\parallel f_i(z_-, v_\parallel, t) + \int_{-\infty}^{-v_{c,-}} dv_\parallel v_\parallel f_e(z_-, v_\parallel, t). \end{aligned} \tag{31}$$

Note that there is no contribution to the electron current from particles with $|v_\parallel| < v_{c,+}$ at $z = z_+$ nor from particles with $|v_\parallel| < v_{c,-}$ at $z = z_-$. This is because the outgoing current of electrons with these speeds is cancelled by the return current of these electrons.

As proposed in [2], we simplify our system by assuming that the parallel current into the wall vanishes individually at each boundary; i.e., $J_\parallel(z_+,t) = J_\parallel(z_-,t) = 0$. Combined with quasineutrality, this imposes $u_e(z_\pm,t) = u_i(z_\pm,t)$. The charge conservation equation (9) can then be integrated to find $u_e = u_i$ for all z.

Our boundary condition on $p_{\parallel,e}$ is chosen based on the physics we intend to model; for the cases considered in this report, we either set $T_e(z_\pm,t) = T_i(z_\pm,t)$ (when ν_{ei} is large) or we assume that the electron temperature is constant throughout the sheath so that $T_e(z_\pm,t) = T_w$ (when we wish to force a Boltzmann electron response), with T_w the temperature of the wall.

5. Normalisations

The normalisations used in the code are given in Table 1.

The normalised drift kinetic equations for ions and neutrals are

$$\frac{\partial \tilde{f}_i}{\partial \tilde{t}} + \tilde{v}_\parallel \frac{\partial \tilde{f}_i}{\partial \tilde{z}} - \frac{1}{2}\frac{\partial \tilde{\phi}}{\partial \tilde{z}}\frac{\partial \tilde{f}_i}{\partial \tilde{v}_\parallel} = -\tilde{R}_{\mathrm{in}}\left(\tilde{n}_n \tilde{f}_i - \tilde{n}_i \tilde{f}_n\right) + \tilde{R}_{\mathrm{ion}}\tilde{n}_e \tilde{f}_n + \tilde{S}_i \tag{32}$$

and

$$\frac{\partial \tilde{f}_n}{\partial \tilde{t}} + \tilde{v}_\parallel \frac{\partial \tilde{f}_n}{\partial \tilde{z}} = \tilde{R}_{\rm in}\left(\tilde{n}_n \tilde{f}_i - \tilde{n}_i \tilde{f}_n\right) - \tilde{R}_{\rm ion}\tilde{n}_e \tilde{f}_n + \tilde{S}_n. \tag{33}$$

The normalised electron fluid equations are

$$\tilde{n}_e = \tilde{n}_i, \tag{34}$$

$$\frac{\partial}{\partial \tilde{z}}\left(\tilde{n}_e\left(\tilde{u}_i - \tilde{u}_e\right)\right) = 0, \tag{35}$$

$$-\frac{\partial \tilde{p}_{\parallel,e}}{\partial \tilde{z}} + \frac{\tilde{n}_e}{2}\frac{\partial \tilde{\phi}}{\partial \tilde{z}} = 0, \tag{36}$$

and

$$\frac{\partial \tilde{p}_{\parallel,e}}{\partial \tilde{t}} + \frac{\partial \tilde{q}_{\parallel,e}}{\partial \tilde{z}} + \tilde{u}_e\frac{\partial \tilde{p}_{\parallel,e}}{\partial \tilde{z}} + 3\tilde{p}_{\parallel,e}\frac{\partial \tilde{u}_e}{\partial \tilde{z}} = \tilde{n}_n \tilde{R}_{\rm ion}\left(\tilde{p}_{\parallel,e} - \tilde{n}_e \tilde{E}_{\rm ion}\right) + \tilde{\mathcal{S}}_{p,e}, \tag{37}$$

where

$$\tilde{\mathcal{S}}_{p,e} \doteq \frac{L_{\rm ref}}{c_{\rm ref}}\frac{1}{2n_{\rm ref}T_{\rm ref}}\mathcal{S}_{p,e}. \tag{38}$$

The zero current boundary condition at the wall, combined with quasineutrality (34) and charge conservation (35), imposes $\tilde{u}_e = \tilde{u}_i$. Note that with these normalisations the electron thermal speed and parallel pressure are related via $\tilde{v}_{{\rm th},e} = \sqrt{2(m_i/m_e)\tilde{p}_{\parallel,e}/\tilde{n}_e}$. Additionally, the electrostatic potential is $\tilde{\phi}(z_\pm, t) = \tilde{T}_e \tilde{v}^2_{c,\pm}$ and $\tilde{T}_e = (m_e/m_i)\tilde{v}^2_{{\rm th},e}$.

Finally, the normalised parallel heat flux is obtained from

$$\tilde{q}_{\parallel,e} = 2\tilde{p}_{\parallel,e}\tilde{v}_{{\rm th},e}\int_{-\infty}^{\infty} dw_\parallel w_\parallel^3 g_e, \tag{39}$$

with the modified distribution function g_e satisfying

$$w_\parallel \tilde{v}_{{\rm th},e}\frac{\partial g_e}{\partial \tilde{z}} + \left(\frac{\tilde{v}_{{\rm th},e}}{2\tilde{p}_{\parallel,e}}\frac{\partial \tilde{p}_{\parallel,e}}{\partial \tilde{z}} + \frac{w_\parallel}{2\tilde{p}_{\parallel,e}}\frac{\partial \tilde{q}_{\parallel,e}}{\partial \tilde{z}} - w_\parallel^2\frac{\partial \tilde{v}_{{\rm th},e}}{\partial \tilde{z}}\right)\frac{\partial g_e}{\partial w_\parallel} = \tilde{G}, \tag{40}$$

and

$$\tilde{G} \doteq \frac{L_{\rm ref}}{c_{\rm ref}}G = \left(-\frac{1}{2\tilde{p}_{\parallel,e}}\frac{\partial \tilde{q}_{\parallel,e}}{\partial \tilde{z}} - w_\parallel \tilde{v}_{{\rm th},e}\left(\frac{\partial \ln \tilde{n}_e}{\partial \tilde{z}} - \frac{\partial \ln \tilde{v}_{{\rm th},e}}{\partial \tilde{z}}\right)\right) g_e. \tag{41}$$

6. Numerical approach

A detailed description of the space and time discretisations employed in the code can be found in report 2047357-TN-14 [5]. Briefly, we employ an explicit time advance algorithm (a strong-stability-preserving Runge-Kutta variant) to evolve the ion and neutral particle distribution functions. A Chebyshev spectral element scheme is used for the spatial discretisation. An iterative method is used to solve the electron energy equation, coupled to the electron kinetic equation. Solution of the coupled equations proceeds schematically in the following way:

normalised variable	definition
$\tilde{t}$	$t(c_{\rm ref}/L_{\rm ref})$
$\tilde{z}$	$z/L_{\rm ref}$
$\tilde{v}_\parallel$	$v_\parallel/c_s$
$\tilde{w}$	w/c_s
$\tilde{n}_s$	$n_s/n_{\rm ref}$
$\tilde{u}_s$	$u_s/c_{\rm ref}$
$\tilde{p}_{\parallel,s}$	$p_{\parallel,s}/(2n_{\rm ref}T_{\rm ref})$
$\tilde{q}_{\parallel,e}$	$q_{\parallel,s}/(2n_{\rm ref}T_{\rm ref}c_{\rm ref})$
$\tilde{T}_s$	$T_s/T_{\rm ref}$
$\tilde{v}_{{\rm th},s}$	$v_{{\rm th},s}/c_{\rm ref}$
$\tilde{\phi}$	$e\phi/T_{\rm ref}$
$\tilde{E}_z$	$eL_{\rm ref}E_z/T_{\rm ref}$
$\tilde{R}_{\rm sn}$	$R_{\rm sn}(n_{\rm ref}L_{\rm ref}/c_{\rm ref})$
$\tilde{R}_{\rm ion}$	$R_{\rm ion}(n_{\rm ref}L_{\rm ref}/c_{\rm ref})$
$\tilde{E}_{\rm ion}$	$E_{\rm ion}/(2T_{\rm ref})$
$\tilde{\nu}_{ei}$	$\nu_{ei}(L_{\rm ref}/c_{\rm ref})$
$\tilde{f}_s$	$f_s(c_s\pi^{1/2}/n_{\rm ref})$
$\tilde{F}_\parallel$	$F_\parallel(L_{\rm ref}/2n_{\rm ref}T_{\rm ref})$
$\tilde{S}_s$	$S_s(L_{\rm ref}\pi^{1/2}/n_{\rm ref})(c_s/c_{\rm ref})$
$\tilde{m}_e$	m_e/m_i
$\tilde{v}_{c,\pm}$	$v_{c,\pm}/v_{\rm th,e}$

reference quantity	definition
$L_{\rm ref}=L_z$	ref. length
$T_{\rm ref}$	ref. temperature
$n_{\rm ref}$	ref. density
$c_{\rm ref}$	$\sqrt{2T_{\rm ref}/m_i}$
m_i	ion mass

Table 1. Definitions for normalised and reference quantities used in the report. Note that $c_s = c_{\rm ref}\sqrt{m_i/m_s}$.

- Solve the ion (32) and neutral (33) drift kinetic equations for f_i and f_n within a Runge-Kutta stage, provided the parallel electric field $E_\parallel$ at the previous time step, and subject to the appropriate boundary conditions (22)-(25).
- With f_i and f_n updated, calculate the ion density and parallel flow, and set $n_e = n_i$ and $u_e = u_i$ at the new Runge-Kutta stage.
- Iteratively solve the coupled equations (37)-(41) for the updated electron distribution g_e and the corresponding heat flux $q_{\parallel,e}$ and parallel pressure $p_{\parallel,e}$. The boundary values for the potential ϕ will be determined such that the moment constraints on g_e are satisfied at the boundaries.

- Solve the electron parallel momentum equation (36) for the parallel electric field $E_\parallel$.
- Repeat.

There are various options for solving the electron kinetic equation (40). We have tried three different possibilities: an iterative method, a shooting method, and a relaxation method. Thus far, none of the methods we have attempted have resulted in a steady-state solution for the electron distribution function. As we have focused primarily on the relaxation method, we describe it along with the numerical difficulties we have encountered.

6.1. Relaxation method

The relaxation method involves adding an artificial time derivative to the electron kinetic equation and evolving it in time until a steady-state solution is obtained. This has two clear advantages: many of the existing techniques for solving the ion kinetic equation can be re-used, and there is no need for repeated construction and decomposition of a large matrix operator as may be the case for an iterative method. The modified, time-dependent electron kinetic equation to be solved is

$$\frac{\partial g_e}{\partial \tilde{t}} + w_\parallel \tilde{v}_{\mathrm{th},e} \frac{\partial g_e}{\partial \tilde{z}} + \left(\frac{\tilde{v}_{\mathrm{th},e}}{2\tilde{p}_{\parallel,e}} \frac{\partial \tilde{p}_{\parallel,e}}{\partial \tilde{z}} + \frac{w_\parallel}{2\tilde{p}_{\parallel,e}} \frac{\partial \tilde{q}_{\parallel,e}}{\partial \tilde{z}} - w_\parallel^2 \frac{\partial \tilde{v}_{\mathrm{th},e}}{\partial \tilde{z}} \right) \frac{\partial g_e}{\partial w_\parallel} = \tilde{G}. \tag{42}$$

This equation is currently solved using an explicit (forward Euler) time advance method, with options to treat the derivatives using either a two-point, upwinded finite difference scheme or the same Chebyshev spectral element scheme employed for the ion and neutral kinetic equations. There is the option to evolve the electron kinetic equation with a fixed $p_{\parallel,e}$ (obtained via explicit-in-time solution of the electron energy equation) or to evolve the energy equation for $p_{\parallel,e}$ in tandem with the kinetic equation.

In the rest of this section, we will discuss some other notable details of the numerical implementation, including treatment of the initial and boundary conditions. We will then describe the current state of the simulation results in the final section.

6.2. Initial condition for g_e

As we seek a solution to the electron kinetic equation that is time-independent (for given values of the ion density and parallel flow), the initial conditions on g_e and $p_{\parallel,e}$ are in principle unimportant. However, choosing an initial condition for g_e with discontinuities or other unsavoury behaviour could potentially lead to numerical instabilities or to g_e going negative over part of the phase space. We have attempted to avoid such issues by choosing a distribution function that smoothly varies from a Maxwellian distribution of velocities at the centre of the domain in z to a Maxwellian with a cutoff velocity at the

walls. The particular form we use is

$$g_e(z, w_\parallel, t=0) = e^{-w_\parallel^2}\left(1 - e^{-b(z-z_-)^2}\tanh\left(a\left(w_\parallel - w_{c,-}\right)\right)\right) \times \left(1 - e^{-b(z-z_+)^2}\tanh\left(-a\left(w_\parallel - w_{c,+}\right)\right)\right), \tag{43}$$

where $w_{c,\pm} = (v_{c,\pm} - u_e(z_\pm))/v_{\mathrm{th,e}}(z_\pm)$ and a and b are user-specified parameters (typically chosen to be 10 and 100, respectively). We then normalise g_e by its zeroth velocity moment. A visual representation of this distribution function is provided in Fig. 1 for a case with $w_{c,\pm} = \mp 1$.

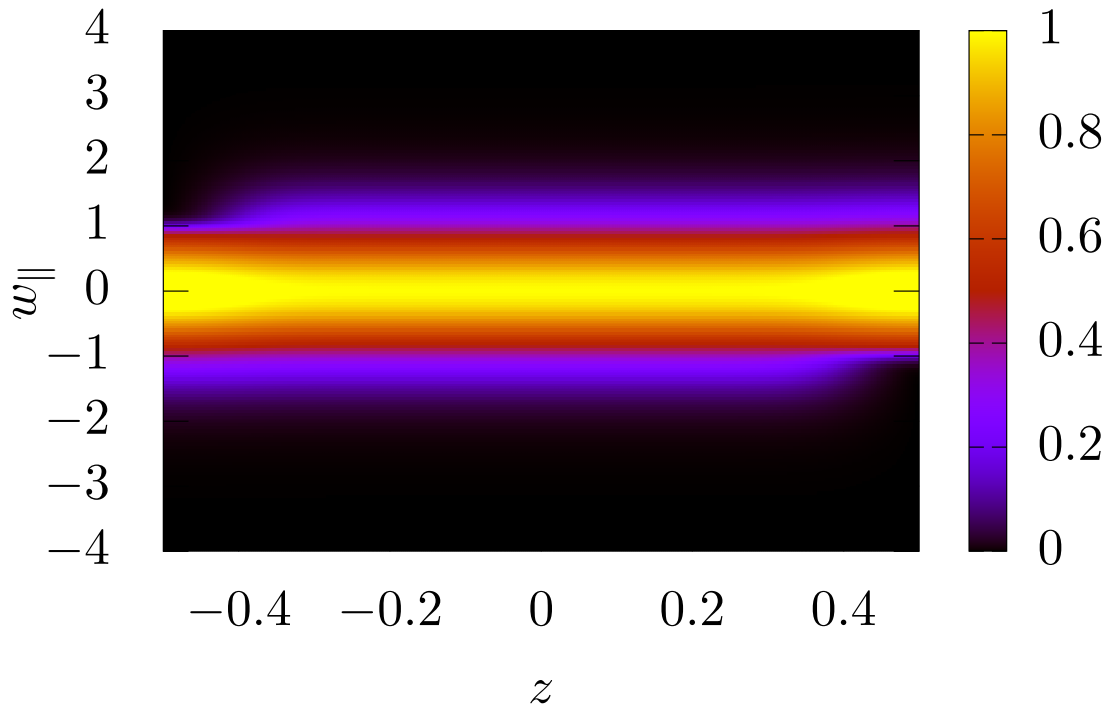

Figure 1. A sample initial condition on g_e, for which $w_{c,\pm} = \mp 1$.

6.3. Enforcing the wall BC

We need to simultaneously ensure that the wall boundary conditions and the integral constraints on g are satisfied. Here's how we do this: First, we interpolate from our $w_\parallel$ grid to one which is symmetric about $v_\parallel = 0$. In practice, we choose to use the same Gauss-Chebyshev-Lobatto grid in $v_\parallel$ that is used in $w_\parallel$. Next construct the distribution function, $g_e^{(0)}$ that is symmetric about $v_\parallel = 0$ via

$$g_e^{(0)}(z_\pm, v_\parallel, t) = \begin{cases} \hat{g}_e(z_\pm, \pm v_\parallel, t), & v_\parallel > 0 \\ \hat{g}_e(z_\pm, \mp v_\parallel, t), & v_\parallel < 0, \end{cases} \tag{44}$$

where $\hat{g}_e$ is the electron distribution function from the previous time step (or iteration, depending on the algorithm used). Then, interpolate back onto the original $w_\parallel$ grid. Next, choose the cutoff speeds $v_{c,\pm}$ – and corresponding electrostatic potentials $\phi(z_\pm, t)$ – to ensure that the moment constraint $\int dw_\parallel w_\parallel g_e^{(1)} = 0$ is satisfied, where we have denoted the distribution function $g_e^{(0)}$ with these speed cutoffs as $g_e^{(1)}$. Finally, we ensure satisfaction of the remaining moment constraints by defining our final distribution function g_e as

$$g_e(z_\pm, w_\parallel, t) = \left(A_\pm + B_\pm v_\parallel^2 \exp\left(-a v_\parallel^2\right) + C_\pm v_\parallel^4 \exp\left(-b v_\parallel^2\right)\right) g_e^{(1)}(z_\pm, w_\parallel, t), \tag{45}$$

where $A_\pm$, $B_\pm$ and $C_\pm$ are constants that will be fixed by demanding that the moment constraints on g_e be satisfied. The form of the velocity-dependent pre-factor is arbitrary, aside from the fact that it should be even in $v_\parallel$ so that the wall boundary condition continues to be satisfied. We have chosen the above form for the velocity-dependence because it is smooth and differentiable (unlike, e.g., terms involving $|v_\parallel|$) and, with appropriate choices for a and b, can maintain positivity of g_e; i.e., in the absence of the Gaussian weighting factors, we found that the modified distribution would be slightly negative at larger $w_\parallel$. In practice, we use $a = 0.1$ and $b = 0.2$. By imposing the moment constraints on g_e, the constants are found to be

$$A_\pm = \frac{1}{G_{00,\pm}}\left(1 + \left(\frac{G_{21,\pm}G_{40,\pm}}{G_{41,\pm}} - G_{20,\pm}\right) B_\pm\right), \tag{46}$$

$$B_\pm = \left(\frac{1}{2} - \frac{G_{02,\pm}}{G_{00,\pm}}\right)\left(G_{22,\pm} - \frac{G_{21,\pm}G_{42,\pm}}{G_{41,\pm}} + \frac{G_{02,\pm}}{G_{00,\pm}}\left(\frac{G_{21,\pm}G_{40,\pm}}{G_{41,\pm}} - G_{20,\pm}\right)\right)^{-1}, \tag{47}$$

and

$$C_\pm = -B_\pm \frac{G_{21,\pm}}{G_{41,\pm}}, \tag{48}$$

with

$$G_{jk,\pm} = \int dw_\parallel v_\parallel^j w_\parallel^k g_e^{(1)}(z_\pm, w_\parallel, t). \tag{49}$$

With these choices, one can verify that

$$\int dw_\parallel \left(1, w_\parallel, w_\parallel^2\right) g_e(z_\pm, w_\parallel, t) = \left(1, 0, \frac{1}{2}\right), \tag{50}$$

as required. An example of this process is illustrated in Fig. 2.

7. Current status

We have tried solving this equation using an explicit (forward Euler) time advance, using both the Chebyshev spectral element scheme employed successfully for the ion and neutral kinetic equations and a two-point, upwind finite difference scheme. We have also tried solving the equation with a fixed $p_{\parallel,e}$ obtained via explicit advance of the electron energy equation and by evolving the energy equation in tandem with the

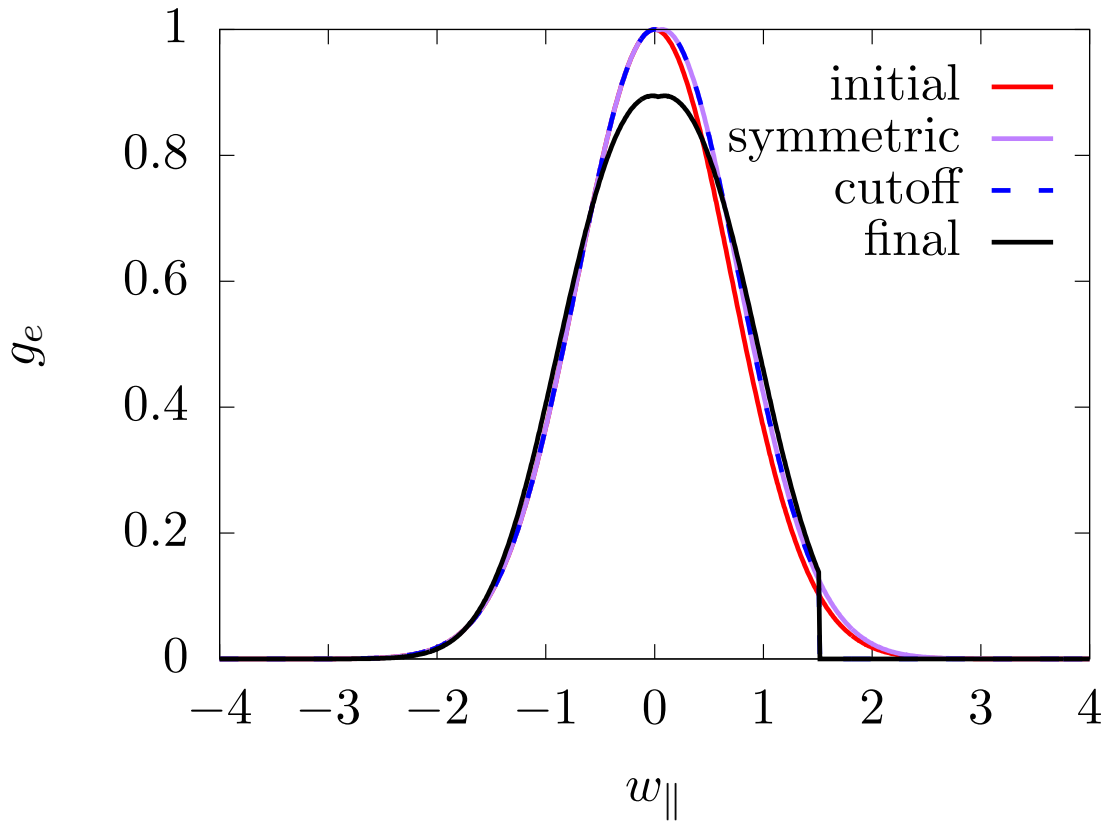

Figure 2. Illustration of the process for ensuring that g_e satisfies both the wall boundary conditions and the moment constraints. Shown in red is the initial distribution at z_-, with the symmetrised distribution in blue, inclusion of the cutoff in purple and the final distribution satisfying all of the constraints in black.

electron kinetic equation. In all cases, we have been unable to find a steady-state solution for g_e at the initial ion-time-scale step. Indicative data showing how the simulations evolve is given in Fig. 3. Generally, we find that the time step required to satisfy the CFL condition for the electron kinetic equation becomes prohibitively small, and this is accompanied by the development of sharp changes in the parallel heat flux at the boundaries in z, followed by sharp changes of the parallel pressure at the boundaries. These oscillations then spread into the rest of the z domain. The distribution function at the boundaries also develop grid-scale oscillations in $w_\parallel$ that originate near $v_\parallel = 0$. Artificial dissipation terms in the form of diffusion in $w_\parallel$ and z have been implemented in the electron kinetic equation, but they do not seem to eliminate these sharp features.

There are numerous possibilities for why we have been unable to obtain a steady-state solution for g_e. We provide a non-exhaustive list here:

- There is a bug in the code. We have tried to minimise the likelihood of this by performing three main tests. First, we artificially set the advection speeds in z and $w_\parallel$ to be independent of z and $w_\parallel$ so that we could solve analytically for g_e (and this test passed). Second, we verified that the time-evolved solution to the electron

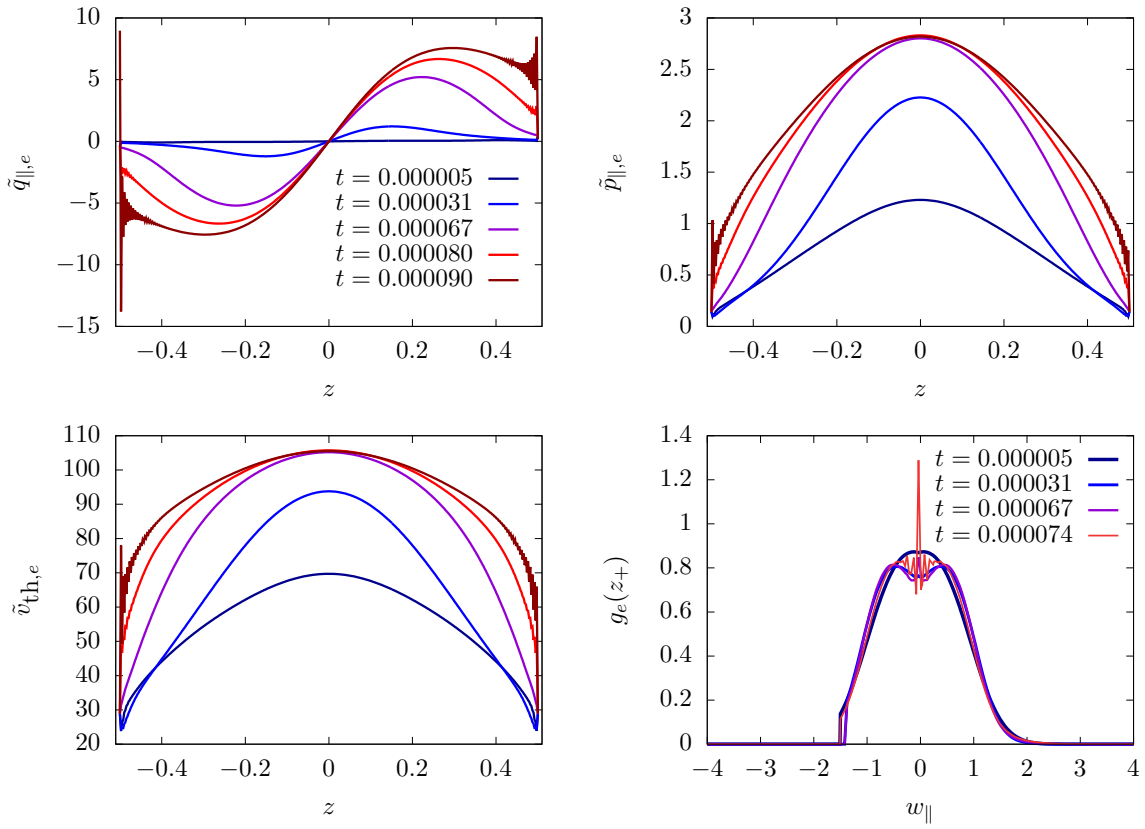

Figure 3. Snapshots showing the evolution of the electron parallel heat flux (top left), pressure (top right), thermal speed (bottom right) and modified distribution function. The three fluid quantities are plotted as a function of location along the field line, z at the same five time slices. The pressure and thermal speed increase in magnitude and develop strong gradients near the boundaries in z before ringing behaviour appears at the boundaries. The modified distribution function g_e at the right boundary in z is shown as a function of $w_\parallel$. The first three time slices are the same as for the fluid quantities, and one can see g_e develop a dip at $w_\parallel = 0$ that is the consequence of forcing a symmetric distribution about $v_\parallel = 0$. The final time slice at which g_e is plotted is earlier than the corresponding slices for the fluid quantities: This is because g_e has already developed grid-scale oscillations around $w_\parallel = 0$ that quickly grow in amplitude as time continues.

kinetic equation satisfies the required moment constraints to within the accuracy of the numerical scheme. Third, we verified that with the appropriate source, a Maxwellian manufactured solution satisfied the steady-state kinetic equation with a residual that decreased with increasing resolution. However, the manufactured solution could not be obtained when initialising with a g_e different from the expected solution.

- Related to the first item, it may be that steady-state solutions for g_e with the specified ion plasma profiles are unstable.
- Another possibility is that the use of fixed profiles for the ion density and parallel

flow prohibit steady-state solutions (or maybe just stable solutions) of the electron kinetic equation with the specified wall boundary conditions. One possible solution for this would be to evolve the ion quantities at the same time as the electron ones, though this would be numerically costly.

- The initial condition on the electron parallel pressure may not be conducive to finding a steady-state g_e, and obtaining such a solution via coupled evolution of $p_{\parallel,e}$ may simply be prohibitively expensive.
- The numerical approach taken to ensure satisfaction of the wall boundary conditions and the moment constraints may be problematic. Fig. 3 suggests this could be the case. Modifications could be made to the procedure described in Section 6.3 to try to improve the robustness of the boundary condition.

As the numerical issues appear to originate at the boundaries, it seems like the natural place to probe next to overcome the numerical difficulties. Ultimately, we should identify the source of the oscillations in the boundary distribution, but an intermediate solution may be to simply smooth the boundary distribution every time step via, e.g., filtering out high frequency components in $w_\parallel$.

[1] F. I. Parra, M. Barnes, and M. R. Hardman. 2d drift kinetic model with wall boundary conditions. *Excalibur/Neptune Report*, 7:2047357–TN–07–02 M1.4, 2021.

[2] F. I. Parra, M. Barnes, and M. R. Hardman. 1d drift kinetic models with wall boundary conditions. *Excalibur/Neptune Report*, 5:2047357–TN–05–01 M1.3, 2021.

[3] S. I. Braginskii. Transport phenomena in a completely ionized two-temperature plasma. *Sov. Phys. JETP*, 6:358, 1958.

[4] M. Knudsen. Das cosinusgesetz in der kinetischen gastheorie. *Annal. Phys.*, 353:1113, 1916.

[5] M. Barnes, F. I. Parra, M. R. Hardman, and J. Omotani. Numerical study of 1+1d drift kinetic models for parallel dynamics in the plasma edge. *Excalibur/Neptune Report*, 14:2047357–TN–14 D2.2, 2022.

[6] `https://github.com/mabarnes/moment_kinetics/blob/electrons/runs/wall%2Bsheath-bc_boltzmann.toml`.

[7] `https://github.com/mabarnes/moment_kinetics/blob/electrons/runs/wall%2Bsheath-bc_braginskii_boltzmann_test.toml`.

[8] `https://github.com/mabarnes/moment_kinetics/blob/electrons/runs/wall%2Bsheath-bc_braginskii_colls.toml`.